Eur. Phys. J. E **19**, 311–317 (2006)
DOI 10.1140/epje/i2005-10060-4

THE EUROPEAN PHYSICAL JOURNAL E

Probing DNA and RNA single molecules with a double optical tweezer

P. Mangeol[1,2], D. Côte[2], T. Bizebard[3], O. Legrand[2], and U. Bockelmann[1,2,a]

[1] Laboratoire de Nanobiophysique, UMR CNRS 7083, ESPCI, 10 rue Vauquelin, 75231 Paris Cedex 05, France
[2] Laboratoire Pierre Aigrain, Ecole Normale Supérieure, 24 rue Lhomond, 75231 Paris Cedex 05, France
[3] Institut de Biologie Physico-chimique, UPR CNRS 9073, 13 rue Pierre et Marie Curie, 75005 Paris, France

Received 7 September 2005 /
Published online: 17 February 2006 –

Abstract. A double-tweezer setup is used to induce mechanical stress in systems of molecular biology. A double strand of DNA is first stretched and the data is compared to precedent experiments to check the experimental setup. Then a short foldable fragment of RNA is probed; the typical unfolding/refolding hysteresis behaviour of this kind of construction is shown and followed by a study of its elasticity and a comparison to a worm-like chain model. Eventually, we describe the unfolding of a larger RNA structure, which unfolds by multiple steps. We show that this unfolding is not reversible and that it presents numerous unfolding pathways.

PACS. 87.15.-v Biomolecules: structure and physical properties – 87.15.He Dynamics and conformational changes – 87.64.-t Spectroscopic and microscopic techniques in biophysics and medical physics

Introduction

Force measurements on single molecules began more than ten years ago, introducing great questions for statistical physics and molecular biology. Experiments on elasticity and structural transitions were done on increasingly complex molecules, such as DNA [1–3], DNA and its complexes with proteins [4,5], or RNA [6,7].

After presenting our experimental configuration based on a double optical tweezer in Section 1, we study the response to mechanical stress on different biological molecules. We first stretch a double-stranded DNA (ds-DNA) to verify our experimental setup in Section 2. Different fragments from 23S ribosomal RNA are then probed in Section 3. A small fragment will allow us to examine the elasticity of a single-stranded RNA and to give an estimation of its persistence length. The study of the reversibility and reproducibility of a bigger fragment unfolding will close this article.

1 Material and methods

There are many setups to measure force on the single-molecule scale [8], the most recent and most precise of which are based on AFM, optical or magnetic tweezers. Our setup is a double optical tweezer; the experimental configuration involves two beads between which one has a biological molecule, and makes it possible to probe molecules on a relevant force range (from 0 to 30 pN), with sub-piconewton resolution.

1.1 Optics: how to obtain two tweezers?

We are using a CW laser beam coming from a titanium-sapphire cavity (Ti:Sa) tunable in the infra-red and pumped in the green thanks to a solid-state laser pumped by laser diodes. To prevent optical elements from undergoing too important heating effects as well as to allow a small overfilling of the objective back focal plane, one starts by widening the laser beam using lenses (L1) and (L2) forming a telescope (Fig. 1). To obtain two independent traps one then splits the beam according to polarization by the association of a half wave plate ($\lambda/2$) and a dichroic cube (C1) in order to obtain two beams of perpendicular polarizations. Before being recombined by a second dichroic cube (C2), one of the two beams is reflected by a mirror mounted on a piezoelectric holder (PZT) in order to deflect it easily from the second. The recombined beams are made enter a high numerical aperture microscope objective in order to make them strongly converge and to obtain two traps. Because of the use of several dichroic mirrors on which beams of perpendicular polarizations may reflect differently, the $\lambda/2$ wave plate is adjusted to ensure equal beam intensities in the plane of the traps.

After their use for trapping, the beams are transmitted through the beads and reflected by an oxidized silicon

[a] e-mail: ulrich.bockelmann@espci.fr

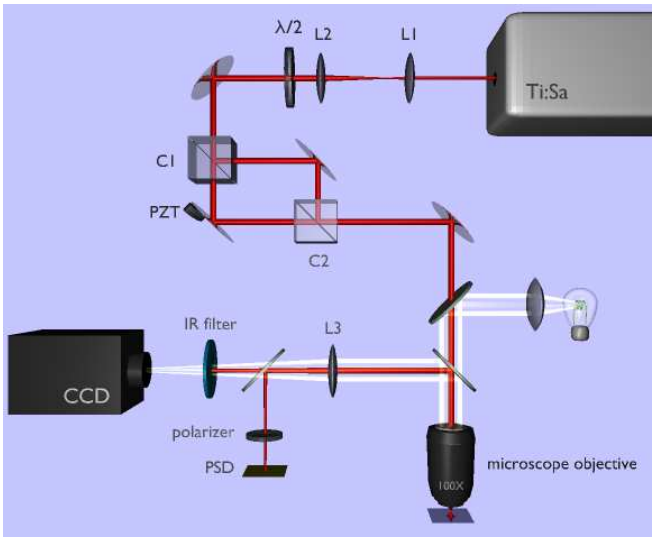

Fig. 1. Schematic of the double-optical-tweezer setup.

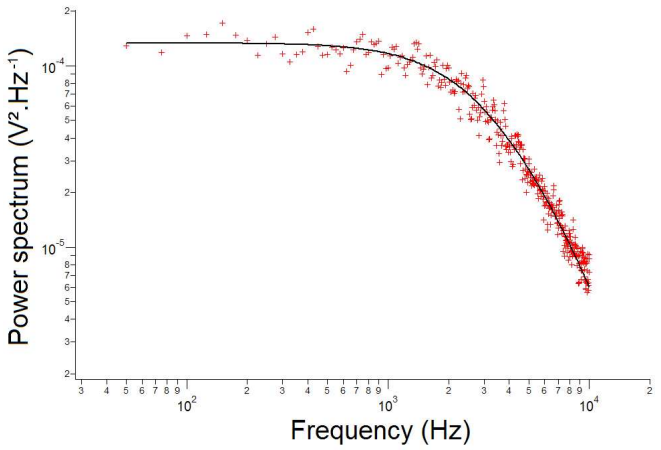

Fig. 2. Position detection signal power spectrum (crosses) and fit from equation (2) (solid line); the cutoff frequency is 2.71 kHz, corresponding to a stiffness of 0.16 pN/nm.

surface, and go back through the microscope objective before being imaged by lens (L3) on a position-sensitive detector (PSD). The use of perpendicular polarizations makes it possible to detect only one beam as the other one is blocked by a polarizer. In order to follow the beads in the biological preparation they are illuminated by a quartz-iodine lamp and imaged on a CCD camera *via* the same microscope objective and lens (L3). As the laser has the same optical path, an absorbing IR filter is placed in order not to saturate the CCD.

1.2 Detection and force measurement

When a trapped bead (with diameter of 1 μm) is pulled by a weak force, in our case a few piconewtons, it moves a characteristic length far smaller than its radius and the laser waist. Thus in practice the deviation angle of the laser beam varies linearly with the bead displacement and thus also with force since at low force the optical trap acts like a harmonic spring on the bead. Even after its reflection and transmission by the microscope objective and lens (L3), the linearity between beam deviation and bead displacement remains true up to the detector. As one of the two beams is absorbed by a polarizer, one bead displacement is measured while its transmitted laser beam deflection is followed by a position-sensitive detector (PSD). The detection system has a time response well suited for calibration in the frequency domain of study.

1.3 Calibration

Optical trapping of particles very small or very large compared to the laser wavelength is well described theoretically by dipolar and geometrical approximations, but apart from these limiting cases there is no complete description and it is necessary to determine applied forces experimentally. Fortunately, the frequency description of a bead movement is well known and described thanks to Langevin theory [9]. A trapped bead immersed in aqueous media will follow the frequency law

$$|X(\omega)|^2 = \frac{k_B T}{\pi^2 \alpha (f^2 + f_0^2)}, \qquad (1)$$

where $X(\omega)$ is the Fourier transform of the axial displacement, k_B the Boltzmann constant, T the temperature, α the drag coefficient of the bead, f the displacement frequency and f_0 the cutoff frequency. This frequency is related to the trap stiffness β by $f_0 = \beta(2\pi\alpha)^{-1}$.

Detection is carried out by an electronic circuit that can be modelled by a low-pass filter, with a cutoff frequency of $f_{el} \simeq 14$ kHz in our case. As the detector voltage signal U is proportional to the particle displacement X, the power spectrum of its Fourier transform takes the form

$$|U(\omega)|^2 = \frac{S_0'}{\left(1 + \frac{f^2}{f_0^2}\right)\left(1 + \frac{f^2}{f_{el}^2}\right)}, \qquad (2)$$

S_0' taking account of the detector sensitivity, *i.e.* the proportionality factor between displacement and voltage. The fit of the experimental curve finally gives us the trap stiffness as $\beta = \frac{f_0}{\alpha}$ (Fig. 2).

2 Force measurement on a single DNA molecule

Force measurements on DNA molecules are of double interest: on the one hand, the mechanical characteristics of this polymer play a central role in some of its functions in the cell, like its folding, replication, recombination, and on the other hand, DNA is a molecule which is rather easy to manipulate, and this makes it a privileged object in polymer physics. Its mechanical characteristics are well known and will be used here in order to check the correct behaviour of the experimental setup.

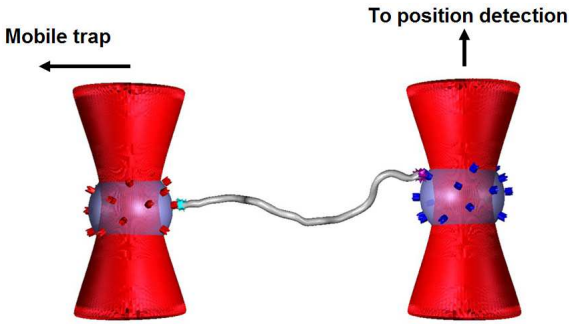

Fig. 3. Schematic view of a DNA molecule streched between two protein functionalized beads.

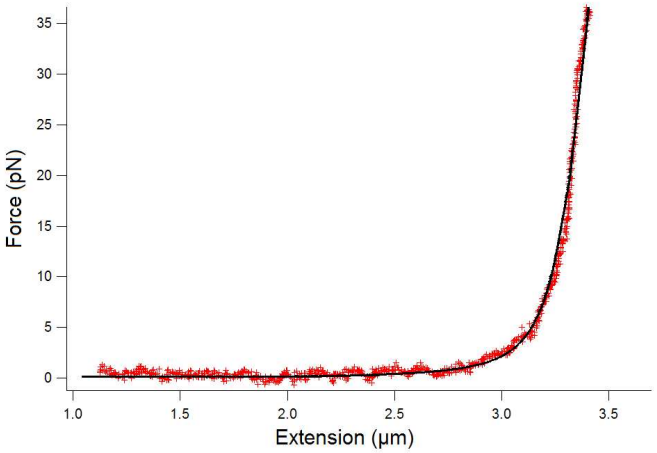

Fig. 4. Force-extension relationship for a double-stranded DNA molecule. Data (crosses) is fitted with the Odijk formula (solid line).

2.1 DNA-beads complex formation

In order to stretch DNA, it is necessary to bind it to macroscopic objects which can be easily handled, like solid surfaces or beads that can be trapped optically or magnetically; here we use silica beads.

One starts by covering these beads with a layer of negatively charged polymer so that DNA does not absorb in a nonspecific and noncontrolled way on the silica surface [10]. Then, in order to have the best control on binding DNA to beads, each end of the DNA is functionalized with a different molecule, one end by biotin and the other by digoxygenin, and beads are functionalized in order to recognize these molecules. One type of bead is functionalized with streptavidin, binding biotin by a strong ligand-receptor noncovalent interaction, and the other one is functionalized with an anti-digoxygenin antibody, thus binding digoxygenin also by a noncovalent but specific interaction.

One forms then DNA-beads complexes by mixing three solutions: a solution containing functionalized DNA, a solution of streptavidin functionalized beads, and a third solution of anti-digoxygenin functionalized beads. This mixture incubates a few hours, and during this time, beads and DNA diffuse and react in order to form complexes where only a few strands are linked to two beads. Just before the experiment this mixture is diluted in a buffer solution ($2\,\mu$L of the mixture in $200\,\mu$L of 10 mM $NaHPO_4$ buffer pH = 7.0). The final solution is a mixture of some DNA-beads complexes with many individual beads.

2.2 Stretching DNA

Now we are ready to stretch DNA-beads complexes thanks to the double tweezer. From an optical point of view the two traps are equivalent, but let us remind that one trap is fixed, the other one mobile, and force measurement is done on the fixed trap (see Fig. 3).

One can find relevant DNA-beads complexes, because of their characteristic movement: the trajectories of two beads linked by a DNA molecule are correlated, whereas after a few seconds of observation unlinked beads move apart by a distance larger than the DNA molecule length. When each bead is near to a trap position, the laser is switched on, and the two beads are trapped in the two tweezers simultaneously. This procedure is successful for molecules longer than $2\,\mu$m.

After a complex is trapped, the principle of the experiment is very simple: by controlling the mobile-trap translation, the two silica beads move apart, each one attached to an end of the molecule which is then stretched. There remains to measure DNA tension thanks to the force it exerts on the fixed bead, and to determine the molecule extension. As we know the imposed distance between the traps, but not the distance between the beads, there remains to subtract the displacement of the beads in their traps. One then simply obtains $d_{beads} = d_{traps} - \frac{2F}{\beta}$, where β is the known trap stiffness. In order to get the molecule length one finally subtracts the radius of each bead.

We chose to study a 10 000 base pair DNA fragment, obtained by PCR from the DNA of λ bacteriophage. A measured force-extension curve is given in Figure 4.

There are several models and several expressions to describe DNA elasticity. The most relevant ones for ds-DNA are based on worm-like chain models [11]. We chose to use the Odijk solution [12], which gives the mean extension $\langle x \rangle$ of the molecule as a function of applied force F:

$$\langle x \rangle = L_0 \left(1 - \frac{1}{2} \left(\frac{k_B T}{F L_p} \right)^{1/2} + \frac{F}{K} \right), \qquad (3)$$

where L_0 is the crystallographic length, L_p the persistence length, K the elastic modulus and T the temperature. The experimental curve fitted with the Odijk model gives the parameters of Table 1. Our fitted parameters are in agreement with the literature values, but the experimental uncertainty is significant. Indeed the stiffness of our traps obtained by calibration is known only with 10% accuracy, and the beads used in the experiment do not necessarily have the same shape and refractive index as those used in the calibration. Because of our specific setup geometry, another important point is that detection depends on the

Table 1. Fit parameters from Odijk model. The literature values come from experiments carried out by other groups for K and L_p under equivalent conditions (PB1X buffer, pH = 7) [11] and the crystallographic length of the chain is obtained by supposing that each base pair has a length of 0.338 nm [13].

Fit parameters	Experimental values	Literature values
K	1000 ± 50 pN	1008 ± 38 pN
L_p	47 ± 5 nm	47.4 ± 1.0 nm
L_0	$3.40 \pm 0.05\,\mu$m	$3.38\,\mu$m

trap height above the reflective surface. Therefore measurements are done at fixed height ($4.0 \pm 0.5\,\mu$m). The experimental uncertainty in this height causes detection signal changes of $\pm 8\%$ [14]. Even if these effects reduce the precision of our results, the setup remains very suitable for the experiments which we will describe thereafter.

3 Force measurement on RNA structures

While the biological importance of RNA has been underestimated for a long time, its catalytic activity and its role in regulation in the cell have made it a major research object over the last 20 years [15]. Even though from a chemical point of view RNA and DNA molecules are very close, RNA is a more difficult object for mechanical studies. First, RNA is less stable because of the omnipresence of RNAase enzymes in a standard laboratory environment. Then, biochemistry of RNA is more difficult, as important techniques like direct chemical synthesis, specific ligation, digestion and enzymatic modifications are much less developed for RNA. Finally, the interpretation of RNA single-molecule measurements are particularly challenging due to the complex sequence-dependent structure and folding processes [7].

We chose to study two RNA fragments from the domain II of 23S *E. Coli* ribosomal RNA (Fig. 5). The first one, which we call RNA *a* in this article, is a 173 nucleotides fragment (consisting of nucleotides 991–1163) and the second one, RNA *b*, is a 735 nucleotides fragment including the first one (nucleotides 529–1263).

3.1 Molecular construction

Force measurement on a RNA fragment requires a particular molecular construction, because usually the two ends of the molecule are very close one to the other, which makes very difficult the direct connection with beads.

In this way, we chose a DNA/RNA hybrid duplex construction. One starts by synthesizing by *in vitro* transcription a 5662 nucleotides long RNA molecule, encompassing the region of interest, located roughly at the middle of the sequence. In addition, ds-DNA molecules with one of their strand partially complementary to the RNA were obtained by PCR. Each one of these strands has a functionalization at its furthest end from the sequence of study: one by a biotin molecule and the other by a digoxygenin molecule. After hybridization of the RNA and the two DNA molecules,

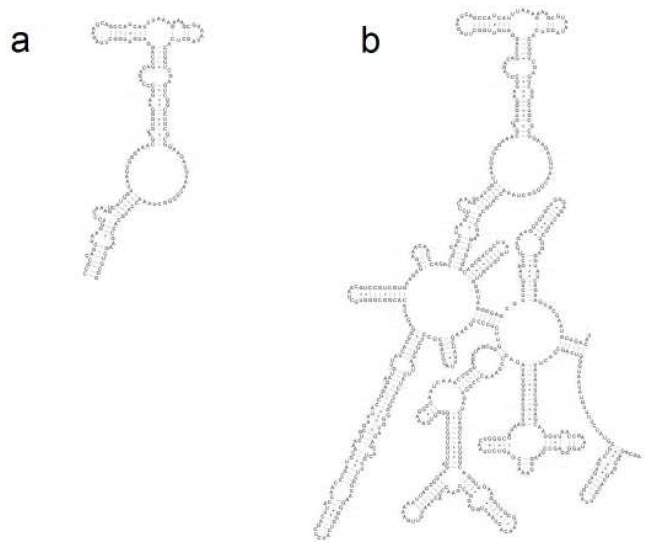

Fig. 5. Secondary structure of the RNA fragments *a* and *b*.

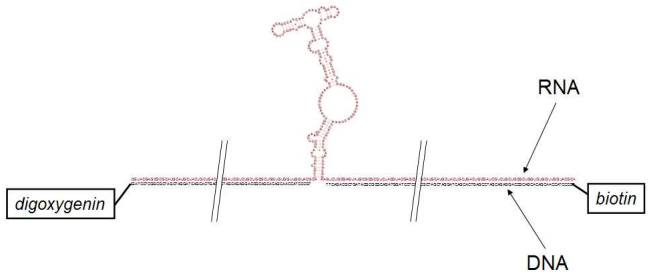

Fig. 6. Schematic view of the RNA/DNA hybrid construction.

one finally obtains a construction (Fig. 6) where the RNA we wish to investigate is flanked by two DNA/RNA "handles", which render the molecule long enough and allow to manipulate it easily.

3.2 Unfolding RNA fragment a

The measurement is done exactly in the same way as the one with DNA: the molecular construction is stretched and the force measurement is done on the fixed bead. We obtain, for example, the force-extension curve of Figure 7. This force-extension curve displays a force drop around 16 pN with an amplitude of approximately 2 pN corresponding to RNA opening and consistent with the force needed to open the DNA helix [3]. We will suppose that during the opening the entire construction is unfolded; this assumption appears rather probable, because we could exert forces up to 20 to 30% higher than the force needed to open the first bases without observing another drop. It is thus not very probable that paired bases remain.

An interesting aspect of this measurement is that it is reversible. By approaching the beads, one observes a drop opposed to the one obtained during the separation (Fig. 7), and also an important hysteresis. Thus folding-up is done approximately 1.5 pN below unfolding where extension is a hundred nanometers smaller. It is important

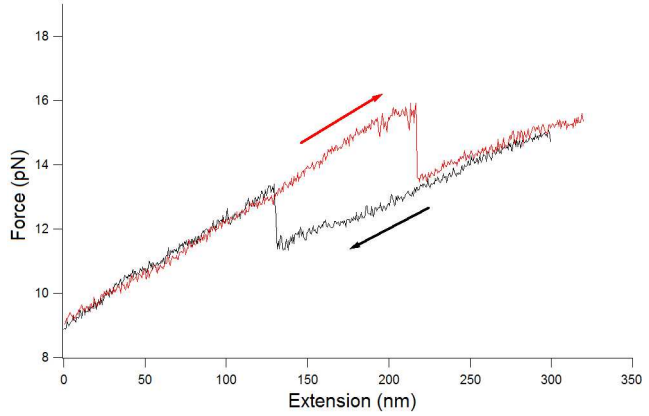

Fig. 7. Force-extension curve on RNA fragment *a* presenting a hystereris between stretching and relaxing.

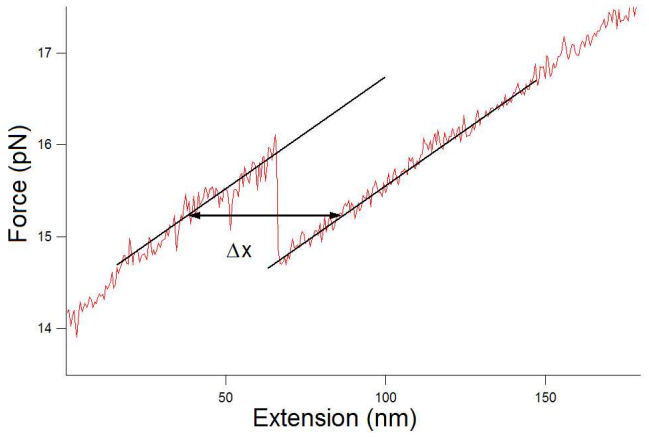

Fig. 8. RNA length measurement principle.

to note that this hysteresis is related to the speed by which the construction is pulled apart, and it seems that one can make it fall considerably by reducing this speed [6]. All experiments shown here are carried out by imposing a speed of $100\,\mathrm{nm\,s^{-1}}$ on the mobile trap.

Let us now extract from the measurements the length changes of the molecular construction caused by unfolding and refolding. For this purpose, we compare the bead positions before and after unfolding or folding at a given force (cf. Fig. 8). At given force the DNA/RNA hybrid tension is constant, and thus its extension is also constant. Thus the positions of the beads before and after unfolding or folding directly give the length of the unfolded RNA. A statistics of the measured length changes is presented in Figure 9. Because of the hysteresis of approximately 1.5 pN, the length measurements obtained during folding and unfolding are separately counted:

$$\Delta L_{unfolding} = 55.7 \pm 9.9\,\mathrm{nm}, \quad \Delta L_{folding} = 51.1 \pm 9.9\,\mathrm{nm}.$$

Although the experimental error is of the order of 20%, one observes that the RNA length during unfolding is more important than the one during folding because the applied force is stronger.

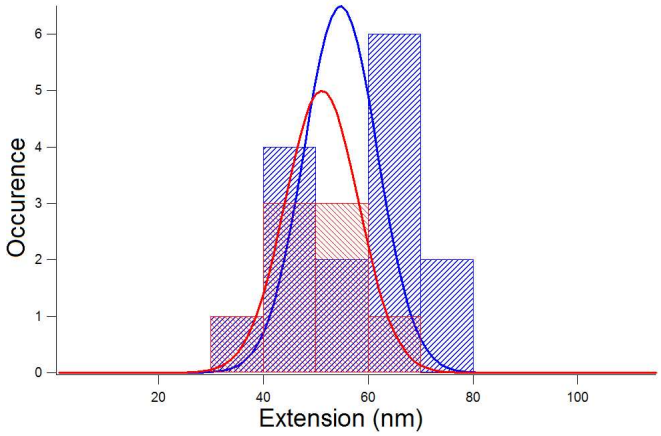

Fig. 9. (Colour online) Histogram of length variation during RNA fragment *a* folding and unfolding (blue: unfolding; red: folding).

We will quantify this effect thanks to a relation proposed by Marko and Siggia [16]. It interpolates a worm-like chain model of polymer elasticity, and has been shown to fit well to mechanical measurements on DNA and RNA. The relation takes the following form:

$$F = \left(\frac{k_B T}{L_p}\right)\left[\frac{1}{4(1-x/L_0)^2} - \frac{1}{4} + \frac{x}{L_0}\right]. \qquad (4)$$

The crystallographic length L_0 is simply given by the fact that each RNA nucleotide has a length of 0.43 nm [17], and that there are 173 nucleotides. Application of this formula enables us to determine the persistence length of single-stranded RNA. A last subtlety in the length estimation of the unfolded RNA fragment is that it is necessary to take into account the distance separating the ends from the chain before unfolding. This distance is given by the diameter of the RNA helix (2.2 nm); the neglect of this geometrical issue would in our case lead to an overestimation of the persistence length by about 3%. We obtain the following persistence length:

$$L_p = 1.1 \pm 0.6\,\mathrm{nm}.$$

This value is in agreement with the literature data, for experiments carried out under equivalent salinity conditions [6].

3.3 Unfolding RNA fragment b

We now turn to our RNA stretching study on a much longer fragment of 23S RNA, which comprises 732 nucleotides. The molecular construction is prepared in the same way as the preceding one. Once more the molecular construction is stretched thanks to optical tweezers, and force is plotted as a function of extension (Fig. 10). Unfolding of this fragment *b* is very different from the one we observed on the smaller fragment *a*. It is noticed first of all that the structure unfolds per piece and not completely in one step, and that the measurement is not reversible

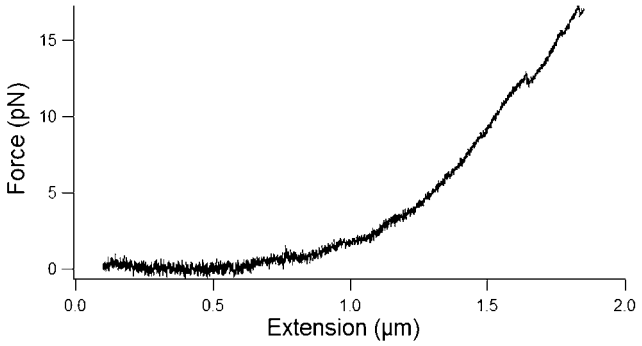

Fig. 10. Force measurement on RNA fragment *b* during strechning.

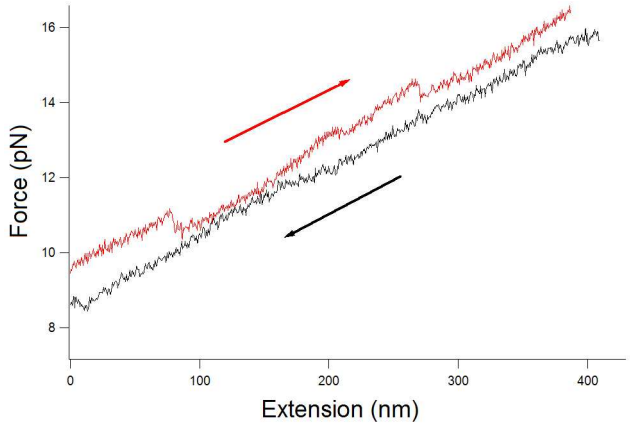

Fig. 11. Force-extension curve on RNA fragment *b*. Data is shown for one fragment during a stretching/relaxing cycle.

(Fig. 11). A second observation is that the force measurement is not as reproducible as the one observed for the short RNA fragment. This observation was already done on similar experiments by the Bustamante group [18] and seems to be partly related to magnesium ion concentration. Indeed Mg^{2+} ions are able to bind together certain parts of RNA by electrostatic interaction, thus playing an important role in the formation of the three-dimensional structure of the ribosome. We thus varied Mg^{2+} concentrations from 0 to 100 mM, but within the experimental uncertainty we did not observe notable dependence of the force curves on the magnesium ion concentration. In the same way, we observed no effect from the ionic strength in the range of 10 to 250 mM of sodium chloride. It is not excluded either that RNA folds differently after each unfolding. The large variety of conformations will then be reflected in the force measurements, and will reveal transitions at different forces and with different amplitudes. However, we observed that in almost 30% of stretchings, the force signal presents two to three transitions distributed between 10 and 16 pN; the other curves present either only one transition at a nonreproducible force, or no transition at all. Some curves are reproducible, but they are isolated cases (Fig. 12).

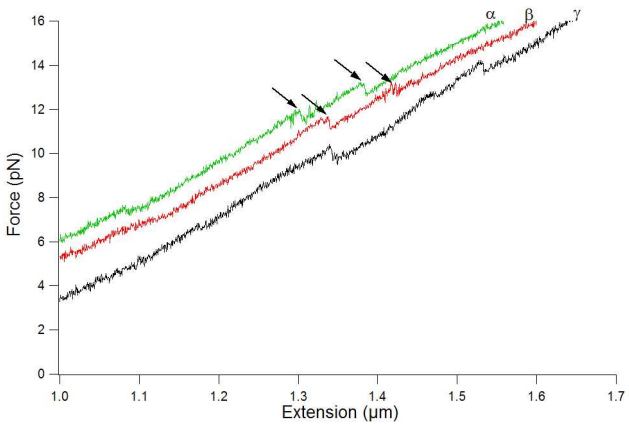

Fig. 12. (Colour online) Green (α), red (β) and black (γ) curves are three successive unfoldings of the same RNA fragment *b*. Curves are translated along the x-axis for a better visualization. Green (α) and red (β) curves show same transitions ($\sim 1\%$ of cases), and the black one (γ) is totally different.

Conclusion

The use of a reflection-type double tweezer makes it possible to probe single molecules, even if the trap height to the reflective surface is an important parameter that has to be carefully controlled. The force-extension curves measured on single DNA molecules enable us to validate the experimental setup. The study of the shortest RNA fragment shows that its unfolding presents hysteresis. Modelling of the measured single-strand elasticity is possible and provides an estimation of the RNA persistence length. The biggest RNA fragment seems to unfold with different transitions. While some structures give quite expected responses [18], the majority of biologically relevant RNAs should unfold in a much more complex way. The unfolding experiments and modelling of highly complex RNA structures may open a door to the determination of unknown structures and their dynamics.

References

1. S.B. Smith, L. Finzi, C. Bustamante, Science **258**, 1122 (1992).
2. S.B. Smith, Y.J. Cui, C. Bustamante, Science **271**, 795 (1996).
3. B. Essevaz-Roulet, U. Bockelmann, F. Heslot, Proc. Natl. Acad. Sci. U.S.A. **94**, 11935 (1997).
4. J.K. Steven, M.D. Wang, Phys. Rev. Lett. **91**, 028103 (2003).
5. U. Bockelmann, B. Essevaz-Roulet, F. Heslot, Phys. Rev. E **58**, 2386 (1998).
6. J. Liphardt, B. Onoa, S.B. Smith, I. Tinoco jr., C. Bustamante, Science **292**, 733 (2001).
7. S. Harlepp, T. Marchal, J. Robert, J.-F. Léger, A. Xayaphoummine, H. Isambert, D. Chatenay, Eur. Phys. J. E **12**, 605 (2003).
8. U. Bockelmann, Curr. Opin. Struct. Biol. **14**, 368 (2004).
9. K. Svoboda, S.M. Block, Annu. Rev. Biophys. Biomol. Struct. **23**, 247 (1994).

10. U. Bockelmann, P. Thomen, B. Essevaz-Roulet, V. Viasnoff, F. Heslot, Biophys. J. **82**, 1537 (2002).
11. M.D. Wang, H. Yin, R. Landick, J. Gelles, S.M. Block, Biophys. J. **72**, 1335 (1997).
12. T. Odijk, Macromolecules **28**, 7016 (1995).
13. W. Saenger, *Principles of Nucleic Acid Structure* (Springer-Verlag, New York, 1988).
14. O. Legrand, D. Côte, U. Bockelmann, *Proc. SPIE*, Vol. **5514** (Dholakia, Spalding, 2004) p. 160.
15. X. Zhuang, Annu. Rev. Biophys. Biomol. Struct. **34**, 399 (2005).
16. C. Bustamante, J.F. Marko, E.D. Siggia, S.B. Smith, Science **265**, 1599 (1994).
17. M.T. Record jr., C.F. Anderson, T.M. Lohman, Quart. Rev. Biophys. **11**, 103 (1978).
18. B. Onoa, S. Dumont, J. Liphardt, S.B. Smith, I. Tinoco jr., C. Bustamante, Science **299**, 1892 (2003).